Research Article Vol. 59, No. 11 / 10 April 2020 / Applied Optics 3417

applied optics

Linear and nonlinear temperature-dependent transmission/absorption characteristics of cadmium telluride crystal for terahertz generation

ARCHANA KUMARI,[1] A. K. CHAUDHARY,[1,3,*] AND M. VENKATESH[1,2]

[1]Advanced Centre of Research in High Energy Materials, University of Hyderabad, Hyderabad 500046, India
[2]The Guo China-US Photonics Laboratory, Changchun institute of Optics, Fine Mechanics and Physics, Changchun 130033, China
[3]e-mail: akcsp@uohyd.ernet.in
*Corresponding author: anilphys@yahoo.com

Received 1 December 2019; revised 4 March 2020; accepted 7 March 2020; posted 9 March 2020 (Doc. ID 366208); published 7 April 2020

This paper reports on the temperature-dependent investigation of linear and nonlinear transmission/absorption characteristics of CdTe crystal in the 300–408 K range using 780–970 nm tunable wavelengths of 140 fs pulses obtained from a Ti:Sapphire laser at 80 MHz repetition rate. The same pulses were also used for terahertz generation. The linear transmission/absorption properties were measured using a specially improvised temperature-tuned spectrophotometer in the 500–1500 nm wavelength range. The linear absorption of 750 nm wavelength gradually increases with respect to a rise in the temperature, and transmission becomes zero at 408 K. Nonlinear absorption induced by femtosecond pulses shows a sudden drop of 18% in transmission above the 800 nm range, due to electron–phonon interaction, which affects the strength of the terahertz signal. It is also responsible for change in the temperature along with the linear shift in the refractive index of the crystal.

https://doi.org/10.1364/AO.366208

1. INTRODUCTION

CdTe is a Group II-VI semiconductor material with excellent optical properties that has attracted the attention of material scientists due to its wide range of bandgap (E_g) between 1.37 and 1.54 eV at room temperature [1–3]. In addition, it possesses strong absorption in the visible region [3,4]. Therefore, it is widely used in different types of scientific applications, such as in fabrication of optoelectronic devices, photovoltaic cells, and as a source for terahertz generation. Since it has a relatively high optical absorption coefficient in the visible region along with good transmission in the 800–1000 nm range [5–7], it is used as an efficient solar cell material as well as potential candidate for terahertz generation using femtosecond laser pulses [8,9]. Moreover, the information of high temperature bandgap energy is very helpful for monitoring of vapor-phase growth of CdTe using optical methods.

Nobel *et al*. reported the spectral transmission of a 0.2 mm thick CdTe wafer at 77 K, whereas Mullins *et al.* extended the temperature study in the 827–1104 K range under argon over pressure. In addition, high temperature bandgap energy was calculated in the 573–1273 K range using high temperature Hall effect measurements [3,10–18]. The bandgap energy is one of the most important parameters used for characterization of semiconductors. It is used in theoretical calculations for showing the significance of these materials in various applications. The intrinsic career density and native defect structure is critically affected at high temperatures because of their dependence on the parameter E_g. The dependence of E_g is widely studied at low temperatures (4–300 K) [13,19]. We have extended our study between the 300 and 408 K temperature range to understand the variation in the value of E_g.

Efficient terahertz radiation can be generated using a femtosecond laser-based optical rectification process from different types of semiconductor and organic materials, such as ZnTe, $ZnGeP_2$, GaAs, GaP, GaSe, CdTe, BNA, and DAST, available in crystal or wafer forms. However, conversion efficiency of the generated terahertz signal is still very low (i.e., $\ll$.001%), which is related to many physical parameters such as transmission/absorption, second-order nonlinearity, surface quality, and damage threshold of these materials. Generally, transmission/absorption data are collected from a tunable spectrophotometer at room temperature. These spectrophotometers have low-powered lamps/laser sources coupled with gratings and provide linear variation in the transmission or absorption data. In addition, a majority of these spectrophotometers provide information at room temperature or up to 343 K (liquid samples). Therefore, it becomes a challenging

task to understand the effect of a continuous-wave source or femtosecond pulses with respect to temperature to know the actual variation in the physical parameters such as transmission/absorption, refractive index, and bandgap. Second, induced absorption by femtosecond pulses is nonlinear in nature and also affects the efficiency of the generated terahertz signal. It is attributed to the variation in the refractive index of the materials with respect to temperature. A small variation in the refractive index also affects the coherence length of the crystal, which is directly linked to the strength of the generated signal. The measured coherence length (l_c) in the current experiment is of the order of 8.6 mm). We have made an experimental attempt to measure the transmission data at tunable wavelengths and ascertained the absorption coefficients of CdTe with respect to temperature at different wavelengths tunable in the 750–1500 nm range [10,11,20–26]. The temperature-dependent refractive index of CdTe was also calculated theoretically along with experimental transmission data to ascertain the absorption coefficient of CdTe. For our study, we have improvised the design of the Lambda 650 spectrophotometer, which has enabled us to measure the reflectance/transmittance data in the 500–1500 nm wavelength range with respect to temperature. An indigenously designed small-sized oven whose temperature was tunable between 298 and 493 K, controlled with +.001 K accuracy, was housed in the spectrophotometer. The measured damage threshold of the CdTe at 140 fs pulses is 280 MW/cm^2. The newly improvised system was able to provide variation in the transmission data of CdTe crystal in the 500–1500 nm range.

The CdTe crystal housed in the same heating system was subjected to 140 fs pulses at 80 MHz repetition rate) tunable between 680 and 1000 nm obtained from a Ti:Sapphire laser (model Coherent Chameleon ultra-II). The results from both experiments clearly reveal the nonlinear absorption behavior of the CdTe crystal. The transmission/absorption data from the above system were used for the calculation of the bandgap energy. Also, it helps us to ascertain the complicated subgap absorption tail called the "Urbach edge," which represents the effect of structural and thermal disorder in the electronic properties of the semiconductor, which is difficult to ascertain theoretically.

In this paper, we have demonstrated the effect of ultrafast pulses on the strength of a generated terahertz signal and its dynamical range, which varies with respect to the incident pump wavelength tunable in the 780–820 nm range. The variation in the linear and nonlinear transmission/absorption clearly indicates the large drop in transmission of the CdTe crystal in the 750–800 nm wavelength range. Further, the shift in bandgap is also corroborated by the rise in the temperature of the crystal, which is once again related to the enhancement in nonlinear absorption. In addition, the present report also helps us to develop new insight into the field of nonlinear optical rectification-based terahertz frequency generation mechanism from different types of pyro-sensitive dielectric materials. Our study also confirms that transmission/absorption data obtained from the spectrophotometer do not provide the actual information about the induced ultrafast thermal lensing effect, change in the coherence length, or dynamics of acoustic phonons modes, which generally occur below the Fermi level at room temperature.

2. EXPERIMENTAL DETAILS

This experiment was performed in three parts: (1) Using femtosecond laser pulses (the commercially available CdTe crystal (M/s Eksma Co.Ltd) and LTGaAs-based PC antennas were employed for generation and detection of terahertz radiation). The thickness and diameter of employed crystal are of the order 0.5 and 15 mm, respectively. The experimental arrangement for terahertz emission and detection is the same as discussed in Refs. [27–29]. The Cherent Chameleon ultra-II (∼140 fs at 80 MHz repetition rate) Ti:Sapphire laser was employed as a laser source in the experiment. It was tunable in the 680–1080 nm wavelength range. The variable attenuator was used to attenuate the power of the incident laser pulse, and the laser beam with selective average power was allowed to incident on the nonlinear crystal, which works as a source of terahertz radiation. The nonlinear crystal was housed in a high precession rotation mount (WP-840-0186) for varying the azimuthal orientation of the crystal. The employed pump and probe powers were of the order of 300 and 75 mW, respectively. The residual pump beam from the CdTe source crystal is eliminated using the combination of Teflon and polyethylene filters. The generated radiation was maximized by azimuthal rotation of the crystal and polarization of laser pulses. The generated terahertz radiation was detected using the photoconductive sampling technique. The generated terahertz radiation from crystals was collimated and focused onto the terahertz detector, i.e., PC antennas (gap ∼5 μm, length ∼20 μm) by two parabolic mirrors. The transmitted portion (probe beam) of laser beam from beam splitter was delayed with respect to terahertz radiation using a motorized translation stage. The probe beam was focused by using another plano–convex lens of focal length 50 cm. The focused probe beam was directed to the detecting antenna and its output was fed to a low-noise current preamplifier connected to the voltage input of the SR830 lock-in. The generated terahertz pulses were measured in a time domain with respect to the probe beam. The temporal profiles were recorded with a 100 ms time constant (i.e., in the lock-in amplifier). (2) The same CdTe crystal was housed in the oven coupled to a temperature controller (Conversion, UK Made). It has an accuracy of +0.01 K. The same setup was also used for femtosecond laser-based transmission/absorption study at different temperatures. The temperature was slowly changed in steps of 5 K per minute in the 298–473 K range. (3) The third part of the experiment was carried out using an improvised version of a Lambda 650 spectrophotometer, which has enabled us to measure the reflectance or transmittance data in the 500–1500 nm wavelength range in the 300–473 K range. The schematic diagram is shown in Fig. 1.

3. RESULTS AND DISCUSSION

Figures 2(a) and 2(b) show the temporal and spectral profiles of the generated terahertz signal from the CdTe crystal.

The terahertz temporal profile of CdTe was measured by selecting incident laser wavelength, tunable between 780 and

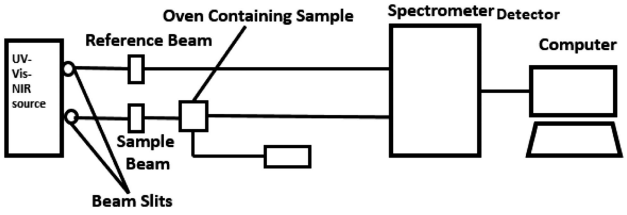

Fig. 1. Schematic diagram of the temperature-tuned spectrophotometer.

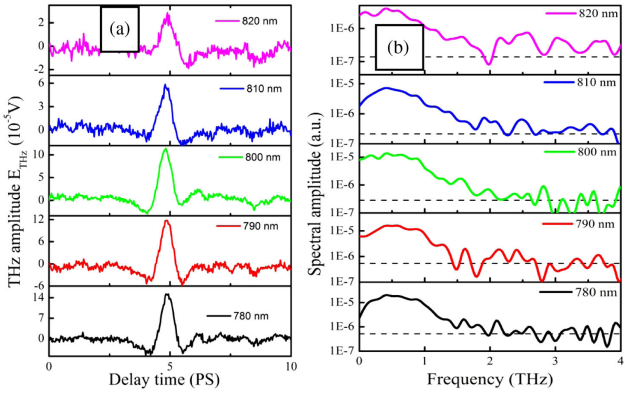

Fig. 2. CdTe. (a) Measured temporal profiles of terahertz radiation with respect to tunable laser wavelengths; (b) spectral profiles of generated terahertz radiation as a function of laser wavelengths.

820 nm at 300 mW power. The measured temporal profiles are shown in Fig. 2(b). The full width at half-maximum is of the order of 0.55 ps, and its peak amplitude decreases with an increase in the incident laser wavelength. Here, the incident photon energy of the laser is selected above the bandgap of the CdTe crystal (i.e., 1.47 eV). The terahertz signal amplitude increases with a decrease in the incident laser wavelength. This may be attributed to the remarkable change of nonlinear susceptibility of the CdTe crystal above and near the bandgap of the material [26]. The spectral amplitude of generated terahertz radiation from the CdTe crystal pumped with 780, 790, 800, 810, and 820 nm wavelengths are 2.01, 1.56, 1.36, 0.75, and 0.48 a.u., respectively. This implies that the emitted spectral amplitude decreases with respect to an increase in the laser central wavelength. Figure 2(b) shows the spectrum of the obtained terahertz radiation is extended up to the 2 THz range. We observed that the crystal has comparatively lower transmission in the 780–820 nm range but provides significant terahertz transmission between 0.1 and 1.2 THz. The lower transmission above 1.2 THz range is due to the higher absorption coefficient of the crystal at room temperature. The effect of the incident laser wavelength on the generated terahertz peak amplitude is illustrated in Fig. 3(a). The emitted terahertz peak amplitude with 780, 790, 800, 810, and 820 nm are 15.2, 11.8, 11.3, 5.84, and 2.85 a.u., respectively. These values clearly imply that the incident laser central wavelength affects the generated terahertz peak amplitude, and it decreases with an increase in laser wavelength. The dependence of terahertz radiation on the incident angle of the laser pulses with respect to the crystal surface normal is shown in Fig. 3(b). The strength of the emitted

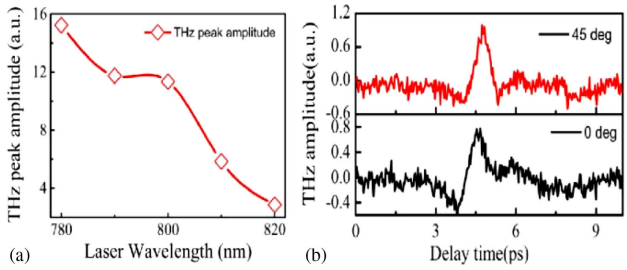

Fig. 3. Dependence of (a) terahertz peak amplitude on laser central wavelength; (b) terahertz radiation on angle of orientation of incident laser pulses.

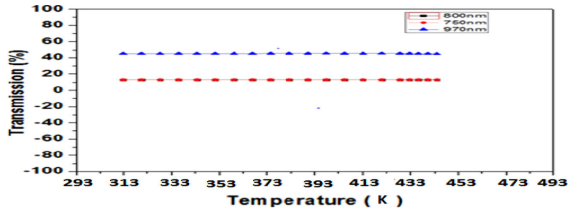

Fig. 4. Temperature versus transmission of CdTe at different wavelengths using femtosecond laser pulses.

terahertz amplitude with 45° angular orientation (9.92 a.u.) is higher than the 0° angular orientation (7.61 a.u.). This is due to the contribution of the surge current (i.e., surface deflection field), coherent phonons, and optical rectification [12,30].

In the second part of the experiment, we have verified the effect of temperature and pulse duration of the femtosecond laser pulse. It was observed that the transmission for 800 and 750 nm wavelengths coincides and reaches 10%, which becomes 0.18% at higher temperatures. However, in the case of a wavelength above 850–970 nm, it reaches 47%, which is much higher than the other wavelengths used for transmission study. The results are shown in Fig. 4.

In order to evaluate the transmittance of the CdTe crystal at room temperature, the power of 750, 800, and 970 nm wavelengths of laser was measured without the sample, which was treated as the reference $I_R(\hbar\vartheta)$. Now same powered wavelengths were passed through the sample crystal housed in the oven holder at different temperatures and measured and treated as $I_S(\hbar\vartheta)$.

Thus, the percentage transmission $T(\hbar\vartheta))$ is defined as

$$T(\hbar\vartheta) = \frac{I_S(\hbar\vartheta)}{I_R(\hbar\vartheta)}. \quad (1)$$

Figure 4 shows the transmission at 750 and 800 nm, which is less than 10% and close to zero at higher temperatures, whereas in the case of 970 nm, it rose to 47%. The reason for this discrepancy could be due to the introduction of nonlinear absorption process in the crystal when subjected to femtosecond laser pulses. The energy absorbed by the crystal during this process is given by the well-known Manoogian–Woley (M–W) equation [3],

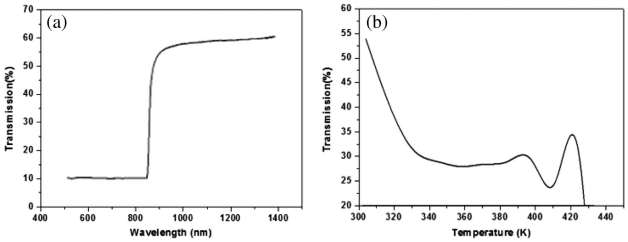

Fig. 5. (a) Wavelength versus transmission and (b) temperature versus transmission of CdTe.

$$E_g = 1.60657 - 5 * 10E(-5) * T - 3.29 * 1E(-2) * \left(\coth\left(\frac{91.5}{T}\right) - 1\right), \quad (2)$$

where the first term represents the initial energy at 4 K, and the second and third terms are related to the lattice thermal vibration and electron–phonon interaction. Electron–phonon interactions includethe Frohlich interaction with longitudinal optical (LO) phonons, deformation-potential interactions with optical and acoustic phonons, and piezoelectric interaction with acoustic phonons [3,31]. The corresponding terahertz frequencies of the LO phonon and acoustic phonon have already been reported in Refs. [3,32,33]. In addition, Frohlich interactions are stronger in the CdTe crystal due to the strong Frohlich coupling constant [34,35]. A further increase in temperature leads to change in the energy (i.e., we observe a shift in the energy that is seen only in the case of femtosecond laser pulses). Thus, it is inferred that it is purely a nonlinear phenomenon. The shift in the energy bandgap proves that all the energy is not used for terahertz generation. This experiment concludes that the incident energy is utilized towards a shift in the energy bandgap (i.e., causes a change in the Fermi energy level). In the second part of the experiment, the crystal was subjected to a modified spectrophotometer, where a specially designed oven whose temperature can be tuned from room temperature to 473 K is introduced in the commercially available Lambda 650 spectrophotometer. The transmission data recorded at room temperature are shown in Figs. 5(a) and 5(b).

The first part of Fig. 5(a) shows a percentage transmission in the 500–1500 nm wavelength range. It is clearly visible that the transmission remains close to zero up to 850 nm, and then it shows a sudden rise and reaches 67.4% at 858 nm. After that, it shows saturation up to 1500 nm. The transmission decreases with an increase in temperature, but it also shows a peak at 380 K, which is followed with a dip at 390 K, followed by another peak at 400 K. These results are shown in the second part of Fig. 5(b). The transmission varies with respect to both wavelength and temperature. A dip is observed in the transmission between 845 and 865 nm wavelength range, which is close to zero, and slowly rises and becomes constant. Here, transmission decreases at 408 K and is almost zero. Thus, we can conclude that the CdTe crystal becomes opaque beyond 408 K.

4. MEASUREMENT OF ABSORPTION COEFFICIENTS AND REFRACTIVE INDEX

The absorption coefficient of CdTe was evaluated using two different methods: one as given in Refs. [2,4]. The second one

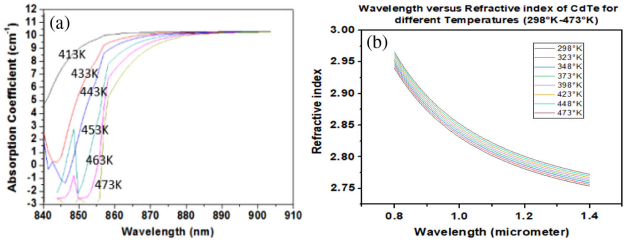

Fig. 6. (a) Absorption coefficient of CdTe at different temperatures and (b) refractive index of CdTe at different wavelengths with respect to temperature.

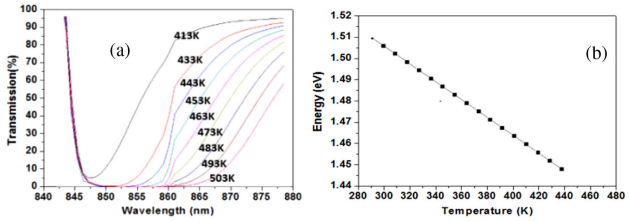

Fig. 7. (a) Experimentally obtained transmission versus wavelength at different temperatures and (b) the temperature versus energy plot of CdTe as obtained by the M–W equation.

is based on femtoseconds laser based transmission/absorption data. The values were found to match using both the methods. Figure 6(a) clearly shows that the absorption coefficient for all wavelengths slowly increases with respect to a rise in the temperature and becomes almost constant. However, the variation in the refractive index is almost linear, even with increasing photon energy, as shown in Fig. 6(b). The refractive index is calculated in the 800–1400 nm (0.8–1.4 μm) range.

5. CALCULATION OF ENERGY BANDGAP (E_g)

The optical energy bandgap was evaluated using the M–W equation because even though this equation is empirical, it has a better physical interpretation at the microscopic level than Varshni's equation. Figure 7(a) shows the variation in the transmission and shift of the cutoff wavelength with respect to temperature, whereas Fig. 7(b) shows the dependence of the bandgap. In Fig. 6, the dependence of the bandgap energy is presented, which is obtained by the M–W equation, as shown in Eq. (2).

This expression matches the accepted value of E_g at 4.2 K and allows us to determine its value at room temperature with an accuracy of +1.5 meV.

The obtained experimental results clearly reveal many interesting linear and nonlinear optical properties of the CdTe crystal, which is not only dependent on temperature, but also on the pulse duration of the laser. The change of temperature either by external means or due to the nonlinear absorption process induced by femtosecond pulses is related to a change in very important physical parameters on the lattice level, which not only changes the refractive index and bandgap, but also influences the process of terahertz generation.

6. CONCLUSIONS

We have successfully demonstrated the effect of laser pulse duration, temperature, and incident laser power on the terahertz generation process from a CdTe crystal. The drop in transmission (∼18%) is being utilized to change the bandgap energy, which in turn causes the Fermi energy level to shift. It is also concluded that the drop in the transmission is mostly due to electron–phonon interaction in CdTe, which also affects the strength of the generated terahertz signal. Finally, the CdTe becomes opaque at 408 K.

Funding. Defence Research and Development Organisation (ERIP/ER/1501138/M/01/319/D(RD)).

Acknowledgment. The authors gratefully acknowledge the financial support provided by the DRDO, Ministry of Defence, and the government of India under ACRHEM Phase III.

REFERENCES

1. M. Krishna, C. Kang, S. Hoon Choi, M. Chen, J. Zhang, X. C. Schleicher, and M. James, "III-VI chalcogenide semiconductor crystals for broadband tunable THz sources and sensors," IEEE J. Sel. Top. Quantum Electron. **14**, 284–288 (2008).
2. R. F. Brebrick and R. Fang, "CdTe I: solidus curve and composition-temperature-tellurium partial pressure data for Te-rich CdTe(s) from optical density measurements," J. Phys. Chem. Solids **57**, 451–460 (1996).
3. G. Fonthal, L. T. Mejia, J. I. M. Hurtado, H. A. Calderon, and J. G. M. Alvarez, "Temperature dependence of the band gap energy of crystalline CdTe," J. Phys. Chem. Solids **61**, 579–583 (2000).
4. E. Belas, E. Uxa Grill, R. Hlídek, P. Šedivý, and L. Bugár, "High temperature optical absorption edge of CdTe single crystal," J. Appl. Phys. **116**, 103521 (2014).
5. G. G. Rusu, "On the electrical and optical properties of nanocrystalline CdTe thin films," J. Optoelectron. Adv. Mater. **3**, 861–866 (2001).
6. B. Li, L. Feng, J. Zheng, W. Cai, Y. Cai, J. Zhang, W. Li, L. Wu, and Z. Lei, "The electrical and optical properties of CSS CDTE thin films deposited in AR+O_2 atmosphere," in *Conference Record of the IEEE Photovoltaic Specialists* (2006).
7. S. Lalitha and S. Z. Karazhanov, "Electronic structure, structural and optical properties of thermally evaporated CdTe thin films," Physica B **387**, 1–2 (2006).
8. A. Kumari, M. Venkatesh, and A. K. Chaudhary, "Terahertz generation from Cadmium Telluride crystal using tunable oscillator laser pulses," in *13th International Conference on Fiber Optics and Photonics*, OSA Technical Digest (online) (Optical Society of America, 2016), paper W3A.6.
9. J. Xie, J. Xu, and X.-C. Zhang, "Terahertz wave generation and detection from a CdTe crystal characterized by different excitation wavelengths," Opt. Lett. **31**, 978–980 (2006).
10. D. J. Olego, J. P. Faurie, S. Sivananthan, and P. M. Raccah, "Single-crystal II-VI on Si single-junction and tandem solar cells," Appl. Phys. Lett. **47**, 1172–1174 (1985).
11. Y. Hwang, Y. Um, H. Kim, G. Jeen, and H. Park, "Temperature dependence of the absorption edge of Cd1-xMnxTe crystals," J. Korean Phys. Soc. **34**, 405 (1999).
12. C. Allahverdi and M. H. Yükselici, "Temperature dependence of absorption band edge of CdTe nanocrystals in glass," New J. Phys. **10**, 103029 (2008).
13. M. M. Choudhury and S. B. Tahmina, "Substrate temperature dependent optical and structural properties of vacuum evaporated CdTe thin films," Eur. Sci. J. **10**, 1857–7881 (2014).
14. J. T. Mullins, J. Carles, and A. W. Brinkman, "High temperature optical absorption edge of CdTe single crystal," J. Appl. Phys. **81**, 6374–6379 (1997).
15. D. T. F. Marple, "Optical absorption edge in CdTe: experimental," Phys. Rev. **150**, 728–734 (1966).
16. J. Camassel, D. Auvergne, H. Mathieu, R. Triboulet, and Y. Marfaing, "Temperature dependence of the fundamental absorption edge in CdTe," Solid State Commun. **13**, 63–68 (1973).
17. S. Abdallah, T. Mohamed, and M. B. Negm, "Photoacoustic characterization of optical and thermal properties of CdSe quantum dots," Eur. Phys. J. Special Top. **153**, 199–368 (2008).
18. A. J. Strauss, "The physical properties of cadmium telluride," Rev. Phys. Appl. **12**, 167–184 (1977).
19. R. K. Willardson and A. C. Beer, *Semiconductors and Semimetals. Vol. 13, Cadmium Telluride* (Academic, 1978).
20. K. L. Chopra and S. R. Das, *Thin Film Sollar Cells* (Plenum, 1983).
21. D. Bonnet, "The CdTe thin film solar cell-an overview," Int. J. Solar Energy **12**, 1–14 (1992).
22. T. L. Chu and S. S. Chu, "Thin film II-VI photovoltaics," Solid State Electron. **12**, 533–549 (1992).
23. R. Bangava, "Optical and photoelectrical properties of GaS and CdTe thin films, components of GaS/CdTe heterojunctions," in *Properties of Wide Bandgap II–VI Semiconductors* (INSPEC, IEE, 1996).
24. D.-E. Arafah and R. Ahmad-Bitar, "Influence of substrate temperature on the processing of CdTe and CdS thin films," Semicond. Sci. Technol. **13**, 322–328 (1998).
25. J. G. Mendoza-Alvarez, J. González-Hernández, and F. Sánchez-Sinencio, "Luminescence and particle size in microcrystalline CdTe thin films," J. Cryst. Growth **86**, 391–395 (1988).
26. J. Sebastian, "The electrical properties of vacuum-evaporated stoichiometric and non-stoichiometric CdTe thin films for opto-electronic applications," Thin Solid Films **221**, 233–238 (1992).
27. M. Venkatesh, K. S. Rao, T. S. Abhilash, S. P. Tewari, and A. K. Chaudhary, "Optical characterization of GaAs photoconductive antennas for efficient generation and detection of terahertz radiation," Opt. Mater. **36**, 596–601 (2014).
28. M. Venkatesh, K. Thirupugalmani, K. S. Rao, S. Brahadeeswaran, and A. K. Chaudhary, "Generation of efficient THz radiation by optical rectification in DAST crystal using tunable femtosecond laser pulses," Indian J. Phys. **91**, 319–326 (2017).
29. M. Venkatesh, S. Ramakanth, A. K. Chaudhary, and K. C. James Raju, "Study of terahertz emission from nickel (Ni) films of different thicknesses using ultrafast laser pulses," Opt. Mater. Express **6**, 2342–2350 (2016).
30. M. Tani, R. Fukasawa, H. Abe, S. Matsuura, and K. Sakai, "Terahertz radiation from coherent phonons excited in semiconductors," J. Appl. Phys. **83**, 2473–2477 (1998).
31. X. B. Zhang, T. Taliercio, S. Kolliakos, and P. Lefebvre, "Influence of electron-phonon interaction on the optical properties of III nitride semiconductors," J. Phys. Condens. Matter **13**, 7053–7074 (2001).
32. A. V. Bragas, C. Aku-Leh, S. Costantino, A. Ingale, J. Zhao, and R. Merlin, "Ultrafast optical generation of coherent phonons in $CdTe_{1-x}Se_x$ quantum dots," Phys. Rev. B **69**, 205306 (2004).
33. M. Schall, M. Walther, and P. U. Jepsen, "Fundamental and second-order phonon processes in CdTe and ZnTe," Phys. Rev. B **64**, 094301 (2001).
34. V. Belinicher, A. L. Chernyshev, and V. A. Shubin, "Single-hole dispersion relation for the real CuO_2 plane," Phys. Rev. B **54**, 14914–14917 (1996).
35. S. S. Islam, S. Rath, K. P. Jain, S. C. Abbi, C. Julien, and M. Balkanski, "Forbidden one-LO-phonon resonant Raman scattering and multiphonon scattering in pure CdTe crystals," Phys. Rev. B **46**, 4982–4985 (1992).